

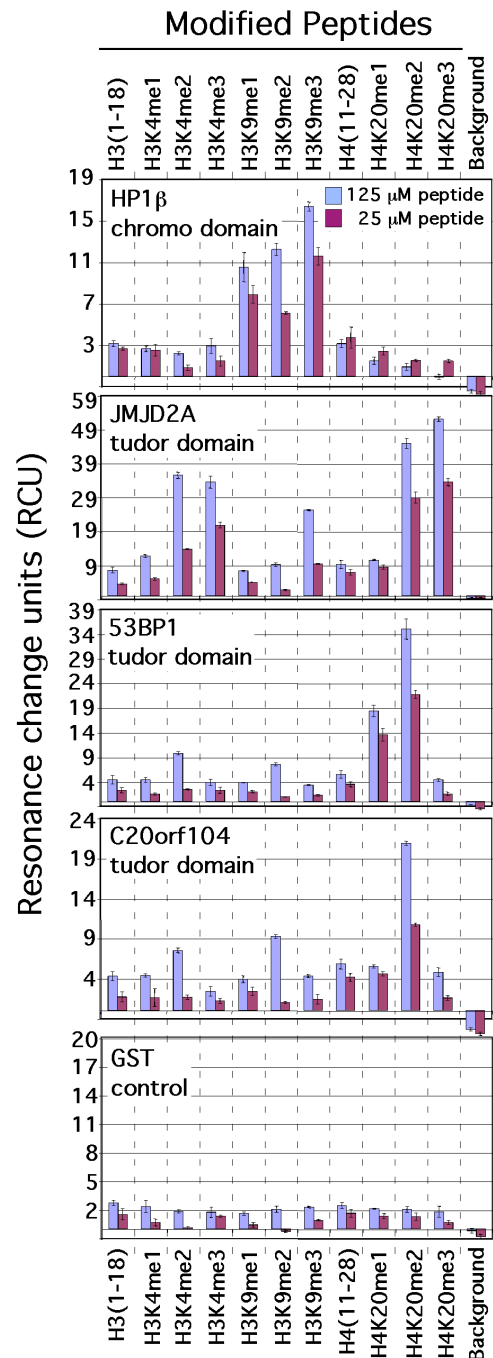
**Tudor domain binding to arrayed peptides confirms the profiles seen on the CADOR chip**

To independently validate the domain-peptide interactions that we detected with the CADOR chip, we used the more traditional approach of surface plasmon resonance (SPR). In this case, instead of probing an array of protein domains with a single labeled peptide, we probed an array of differentially modified peptides with a single domain. A peptide array was generated with the nine modified peptides used to probe the domain array. Unmethylated control peptides were also included. We first demonstrated that the chromo domain of HP1 $\beta$  binds specifically to the methylated H3K9 motif (**Fig S1**). We then probed the Flex Chip with the tudor domains (JMJD2A, 53BP1 and C20orf104) that we had detected as methyl-dependent histone tail binders. This approach allows us to judge the relative binding affinity of a tudor domain with the arrayed peptide set. The JMJD2A binds most strongly to H4K20 in the di- and trimethylated states. It also binds H3K4me<sub>2</sub>, H3K4me<sub>3</sub> and H3K9me<sub>3</sub>. Using this approach, the tudor domains of 53BP1 bind strongly to H4K20 in the mono- and di-methylated states. Weak binding of 53BP1 tudors is also seen with H3K4me<sub>2</sub> and H3K9me<sub>2</sub>. The C20orf104 tudor again displays a binding profile similar to that of the 53BP1 tudors, with selective binding to di-methylated peptides (H3K4me<sub>2</sub>, H3K9me<sub>2</sub> and H4K20me<sub>2</sub>). Thus, using this approach (**Fig S1**), we confirmed the specific tudor domain interactions first detected on the CADOR chip (**Fig 2**) and observed by the pull-down experiments (**Fig 3**).

**METHODS - Surface Plasmon Resonance**

Peptide-protein interactions were evaluated using HTS Biosystems' (East Hartford, CT) FlexChip Kinetic Analysis System that utilizes grating-coupled SPR microarray technology. Biotinylated peptides derived from histone tails were diluted to 125  $\mu$ M and 25  $\mu$ M in 1X PBS + 50  $\mu$ g/ml BSA. These were spotted on a neutravidin coated affinity chip in triplicate spots using a Cartesian pin contact arrayer, then sealed with a fluid tight flowcell. The array was blocked with 1X PBS, 0.5% Tween, 1:10 Superblock (Pierce) and 1 mM d-biotin (Sigma) and then sequentially followed with (1) running buffer (1X PBS + 0.5% Tween) for 30 minutes of equilibration, (2) GST fusion protein resuspended in running buffer at a set concentration for 60 minutes of sample association, and (3) running buffer alone for 30 minutes of sample dissociation. Specific binding to each spot results in a change in mass locally. This was recorded simultaneously for all spots in real time by measuring SPR change using a CCD camera during the entire run. Resonance changes between the onset and the end of the sample association phase were calculated as end-point values for each spot using the FlexChip Data Analysis software.

**Supplementary Figure 1.** A surface plasmon resonance based approach detects methyl-dependent interactions of tudor domains with arrayed peptides from histone tails. The proteins were diluted to the following concentrations: HP1beta to 1  $\mu$ M, JMJD2A to 5  $\mu$ M, 53BP1 to 10  $\mu$ M and C20orf104 to 25  $\mu$ M. A control sample of GST fusion protein alone was also compared at 25  $\mu$ M. The protein samples were allowed to flow over a chip spotted with biotinylated peptides at two concentrations (25  $\mu$ M and 125  $\mu$ M). The background spot was comprised of the peptide diluent only. Binding was quantitated by measuring the change in surface plasmon resonance units over each spot following 60 minutes of sample flow over the chip. Data from 3 replicate spots was averaged to show the resonance change units (RCU) measurement for each peptide as a histogram and the corresponding standard deviations depicted as error bars.



**Supplementary Figure 2.** Western analysis was performed with methyl-specific antibodies to confirm the presence of different methyl marks on the core histones. Western analysis was performed with the following specific antibodies; H3 (Upstate Cat# 06-755), H4 (Upstate Cat# 07-108), H4K20me3 (Upstate Cat# 07-463) and H3K4me3 (Upstate Cat# 07-473).

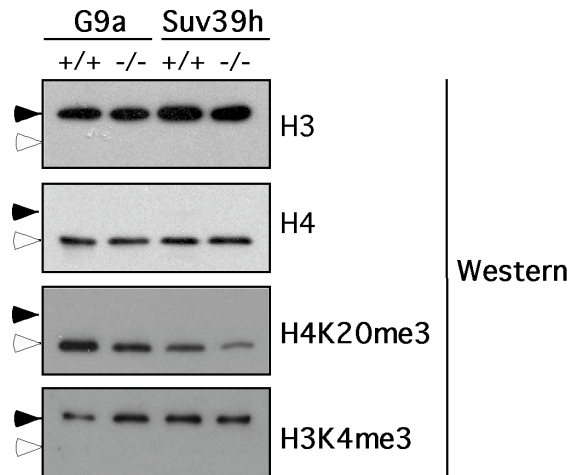


**Table S1. Details on subcloned domains – accession numbers and regions cloned.**

<b>Protein</b>	<b>Region</b>	<b>Accession</b>	<b>Protein</b>	<b>Region</b>	<b>Accession</b>
<b>TUDOR</b>			<b>PhD+</b>		
A1	ESET (218-436)	NP_036564	G1	JMJD2A PhD+ 2Tudor (682-1047)	NP_055478
A2	CG1-72 (54-160)	NP_057102	G2	JMJC PhD (682-865)	NP_055478
A3	FX (56-152)	AAH67272	G3	M96 Tudor+PhD (1+298)	AAH10013
A4	C20orf140 (85-129)	NP_057520	G4	MYST4 PhD+PhD (165-359)	AAH48199
A5	JMJD2A/2 (944-1047)	NP_055478	G5	NSD1 PhD+PWWP (1237-1645)	Q96L73
A6	Pombe 1 (25-162)	CAA22823	G6	WHSC1 PhD+PWWP (780-1016)	NP_579877
A7	Pombe 2 (620-789)	CAB39904	G7	PRKCB1 PhD+BRD+PWWP (75-393)	Q9UIU4
A8	Colon 1 (65-159)	AAC18034	G8	BS69 PhD+ BRD (1-392)	AAH12586
A9	Colon 2 (275-364)	AAC18034	<b>CHROMO</b>		
A10	JMJD2A/1 (856-966)	NP_055478	H1	TIP60 (1-77)	AAB18236
A11	Tudor 9 (628-757)	NP_694591	H2	CHD2 (247-358)	AAB87382
A12	LaminB (1-78)	NP_919424	H3	CHD4 (503-591)	AAH38596
B1	TDRD1/1 (75-222)	NP_112568	H5	SMARCC2 (179-256)	AAH26222
B2	TDRD1/2 (695-846)	NP_112568	H6	MRG15 (1-80)	AAD29872
B3	TDRD2 (292-433)	NP_006853.1	H7	RBBP1 (41-91)	AAD41239
B4	TDRD3 (495-651)	Q9H7E2	H8	PC2 (1-75)	AAH80718
B5	TDRD4-1 (1-104)	Q9NUY9	H9	PC3 (1-71)	AAG09180
B6	TDRD4-2 (220-358)	Q9NUY9	H10	CHD5 (260-430)	AAK56405
B7	TDRD4-3 (405-571)	Q9NUY9	I1	MI-2 (480-539)	CAA60384
B8	TDRD5 (103-253)	Q8NAT2	I2	HP1 alpha (1-120)	P45973
B9	PCTAIRE-1 (449-591)	NP_055105	I3	HP1 gamma (11-129)	NP_057671
B10	PCTAIRE-2 (639-787)	NP_055105	I4	Msl3-like (1-103)	AAD38499
B11	PCTAIRE-3 (896-1038)	NP_055105	I5	SUV39H1 (1-114)	AAB92224
B12	JMJD2A/1-2 (856-1047)	NP_055478	I6	CBX1 (1-52)	AAD21972
C1	EBNA-2Co-A (635-788)	NP_055205	I7	HP1 beta (1-185)	P23197
C2	Ret-bp1 (36-138)	AAB28543	I8	CDY1 (1-71)	AAD22735
C3	M96 (25-115)	AAH10013		TUDOR	
C4	STK31 (57-153)	Q9BXU1	J1	L(3)MBT (430-539)	NP_056293
C5	53BP1/1-2 (1459-1634)	NP_005648	J2	SCML1 (41-477)	NP_057413
C6	53BP1/1 (1459-1587)	NP_005648	J3	SCML2 (57-261)	AAH64617
C7	53BP1/2 (1518-1634)	NP_005648	J4	SCMH1 (1-193)	AAH21252
C8	Anchor (690-849)	NP_003479	J5	LML2 (201-620)	Q969R5
C9	2B (895-1060)	NP_055830	J6	KIAA1617 (267-496)	XP_166140
C10	2C (849-1017)	NP_055876	J7	C20orf140-MBT (1-83)	NP_057520
C11	RBP1 like-2 (34-130)	NP_112739	J8	CG1-72-MBT (1-74)	NP_057102
C12	SMN (80-172)	NP_075012	J9	C20orf140-MBT+TDR (1-194)	NP_057520
<b>CW</b>			<b>BROMO</b>		
D1	CW1 (451-545)	BAA74875	K1	GCN5 (1364-1624)	Q92830
D2	CW3 (117-194)	AAH02725	K2	TAF1- D1 (1364-1499)	NP_620278
D3	CW4 (346-438)	CAD23056	K3	TAF1- D2 (1486-1624)	NP_620278
D4	CW5 (405-472)	BAA09485	K4	P/CAF (709-832)	S71788
D5	CW6 (14-88)	XP_087384	K5	SP140 (739-866)	NP_009168
D9	Tudor Rhp9 (341-510)	CAB46775	K7	SNF2 beta (1449-1565)	S45252
<b>PWWP</b>			K8	SMAP (588-721)	NP_899203
E1	BRPF1 (1073-1220)	AAH53851	K9	BAF180 1-2 (30-301)	NP_060635
E2	BS69 (151-343)	AAH12586	I10	BAF180 3 (335-481)	NP_060635
E4	DNMT3B (107-341)	Q9UBC3	K11	BAF180 3-4 (335-481)	NP_060635
E5	HDGF (1-113)	P51858	K12	BAF180 5-6 (660-862)	NP_060635
E6	HRP-3 (1-114)	BAA90477	L1	TIF1 alpha (847-973)	AAD17258
E7	MSH6 (72-216)	P52701	L2	KAP-1 (685-835)	AAB37341
E8	NSD1 (1736-1871)	Q96L73	L3	P300 (1075-1203)	NP_004371
E9	WHSC1-1 (205-349)	NP_579877	L4	WDR9 1-2 (1145-1429)	Q9NSI6
<b>SANT/SWIRM</b>			L5	WDR9 1 (1145-1277)	Q9NSI6
F1	MPP11-like (493-593)	XP_379909	L6	WDR9 2 (1305-1429)	Q9NSI6
F2	MTA1 (267-353)	Q13330	L7	BAZ (1327-1483)	NP_075381
F3	N-CoR2 (408-680)	Q9Y618	L8	BRDT 1-2 (15-388)	AAH62700
F4	N-CoR2-1 (408-489)	Q9Y618	L9	BRDT 1 (15-145)	AAH62700
F5	N-CoR2-2 (598-680)	Q9Y618	L10	BRDT 2 (258-388)	AAH62700
F6	N-CoR1 (416-695)	NP_006302	L11	BRD4 1 (45-165)	NP_932762
F7	RERE (304-400)	AAH62342			
F8	ADA2-SANT (55-144)	NP_001479			
F9	Zuotin Rel. (402-593)	XP_168590			
F10	KIAA1915 (248-390)	BAB67808			
F11	KIAA0601 (207-391)	CAB72299			
F12	ADA2-Swirm (337-443)	NP_001479			